International Journal of Microwave and Wireless Technologies, 2010, 2(2), 203–209.
doi:10.1017/S1759078710000310

Spectrum optimization in ultra-wideband systems

ELENA PANCERA[1], JENS TIMMERMANN[2], THOMAS ZWICK[1] AND WERNER WIESBECK[1]

In this paper the non-ideal and frequency-dependent behavior of the hardware components of the ultra-wideband (UWB) transmitter RF-front end is analyzed. Both digital and analytical methods to compensate for this frequency-dependent behavior are investigated, in order to optimize the radiated wave, so that its spectrum perfectly matches the given mask. An example of spectral system optimization with analog devices is shown and verified through measurement results.

Keywords: Ultra-wideband, Non-idealities, Shaping filter, RF front-end

Received 10 October 2009; Revised 15 February 2010; first published online 27 April 2010

I. INTRODUCTION

Ultra-wideband (UWB) has emerged in the last years from a mainly basic research area toward a more application-oriented topic. UWB is a relatively new wireless technology, which is characterized by the usage of a very large frequency band and low transmission power. A first regulation of the frequency spectrum for UWB communications has been issued in 2002 by the Federal Communications Commission (FCC) in the USA. It has allocated a frequency interval of 7.5 GHz in the 3.1–10.6 GHz frequency band for UWB commercial applications [1]. Recently (February 2007), also the European Union (EU) has approved the usage of a frequency spectrum for UWB communications allocating a band of 2.5 GHz from 6 to 8.5 GHz for UWB operations [2]. An additional band (3.4–4.8 GHz) can be used for particular applications with very low duty cycles. In both the FCC and EU UWB regulations, the radiated power spectral density (PSD) is limited to a maximum of −41.3 dBm/MHz in the UWB band, in order to avoid interference with other devices.

Thanks to its peculiarities, UWB is a powerful solution in many fields. In particular, the huge bandwidth allows for the achievement of a high data rate with applicability for multimedia applications. Moreover, high resolution can be achieved, which is an advantage for localization in the radar field and also for medical applications. Furthermore, also sensor networks can benefit from the huge bandwidth, which allows for high user density [3].

UWB research activities and knowledge are widely spread all over the world and they are both component oriented and with a system engineering focus. In literature there are many contributions dealing with hardware components, such as antennas and antenna arrays, filters, etc. Moreover, also many publications regarding propagation effects, channel modeling, etc., and system analysis and design can be found.

Together with component design and system design, an important topic to be investigated in the UWB case is the system optimization. Differently from narrow band systems, in the UWB case the devices (antennas, arrays, filters, antennas integrated with filters, etc.) have to show a behavior, which is not frequency dependent, in order to not distort the signal and hence lower the overall system performance.

An important aspect to be underlined is that in the UWB regulations the transmitted signal has to satisfy the given mask. It has to be noted that the mask limits the transmitted PSD instead of the total amount of the transmitted power. Hence a maximization of the total radiated power is necessary in order to completely exploit the power allowed to be transmitted. Moreover, due to the system non-ideal behavior, i.e. because of its frequency dependence, even if the signal spectrum satisfies the given mask, the fulfillment of the mask itself is not guaranteed. This means that not all the power, which is allowed to be transmitted, is effectively radiated. This is due to a frequency-dependent behavior of the UWB RF components (such as antennas) and also to the fact that the pulses created by the effectively used pulse generators have high-energy content at low frequencies. Hence, their energy content cannot be assumed constant with the frequency in the UWB band.

In literature, different methods have been proposed in order to create signals that fulfill the given mask at most. The majority of these methods consists in generating a particular pulse, which perfectly matches the given mask [3–6]. Other methods consist in applying a bandpass filter before the antenna [7–9]. However, these techniques do not take into consideration the effect of the frequency dependence of the transmit antenna and of the fact that it differentiates the radiated pulse [10] and consequently they are suboptimal. In [11] the authors have presented a method to improve the spectrum fulfillment of the radiated signal, which compensates also the effect of the frequency-dependent antenna behavior.

In this paper, the causes of non-idealities at the UWB transmitter RF-front end are analyzed, taking into account

[1]Institut für Hochfrequenztechnik und Elektronik (IHE) – Karlsruhe Institute of Technology (KIT), Kaiserstrasse 12, 76131 Karlsruhe, Germany. Phone: +49-721-608-6267; Fax: +49-721-691-865.
[2]EADS Astrium – Claude Dornier Strasse, 88090 Immenstaad am Bodensee, Germany.
Corresponding author:
E. Pancera
Email: elena.pancera@kit.edu

their impact on the distortion produced on the signal. Moreover, methods to compensate the signal distortion in order to improve the spectrum of the transmitted signal are investigated. The applicability and the performance of these methods are regarded.

The paper is organized as follows. In Section II the non-idealities in the UWB RF-front end are investigated, with a mathematical description of the UWB radio link. In Section III the methods for spectrum optimization are regarded. In Section IV an example of spectrum optimization is shown and validated through measurement results.

II. NON-IDEALITIES IN THE UWB RADIO LINK

A UWB transmitter is composed, in the simplest way, by a pulse generator and a transmit antenna, as shown in Fig. 1, where $p(t)$ is the pulse at the output of the pulse generator, $h_A(t)$ the impulse response of the transmit antenna [10], and $e(t, r)$ the radiated electric field at a distance r from the transmitter. Both the pulse generator and the antenna contribute, due to their frequency-dependent behavior, to distort the signal, as it is illustrated in the following.

A) UWB pulse generators

The pulses created by the effectively used pulse generators have high-energy content at low frequencies, and hence they are not perfectly matched to the required mask. Even in the ideal case of an antenna with a frequency-independent transfer function in the UWB frequency range, the non-constancy of the generated pulse causes a worsening of the system performance, since not all of the allowed power is transmitted. In Fig. 2 the normalized measured frequency spectrum of a commercially available pulse generator (PSPL 3600 [12]) is shown. It can be easily seen that the power spectrum of the generated pulse is highly frequency dependent.

B) UWB antennas

The frequency domain behavior of a UWB antenna is usually characterized through its transfer function $H_A(f)$, from which the antenna gain can be derived [10]. The frequency dependence of $H_A(f)$ causes a distortion of the spectrum of the radiated signal.

As an example, the transfer function of a Bow-tie antenna (36×31 mm^2, see Fig. 3 [18]) is shown in Fig. 4.

Hence, the presence of the antenna, which in the practical case has a transfer function and hence a gain is frequency dependent, causes the transmitted signal to be distorted and not to completely fulfill the given mask.

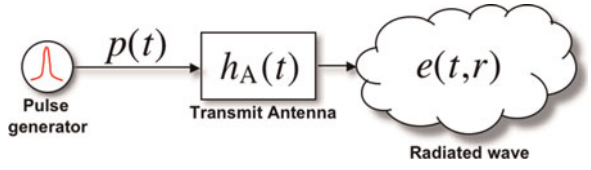

Fig. 1. Block scheme of the transmitter (time domain representation).

Fig. 2. Normalized measured spectrum of the signal created by a PSPL 3600 pulse generator.

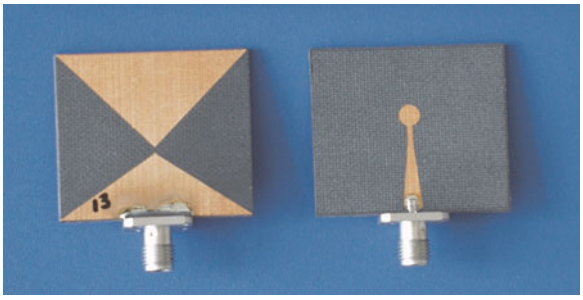

Fig. 3. The investigated Bow-tie antenna (dimensions: 36×31 mm^2): front and rear sides).

C) UWB radio link

The effect of the frequency-dependent behavior of both the generated pulse and the antenna can be investigated regarding the UWB radio link. According to Fig. 1, the radiated electric field $e(t, r)$ at a distance r from the transmitter can be written as [10, 13]

$$e(t, r) = \underbrace{\frac{1}{r}\delta\left(t - \frac{r}{c_0}\right)}_{h_{Ch}(t,r)} * h_A(t) * \frac{1}{2\pi c_0}\frac{\partial}{\partial t}p(t), \qquad (1)$$

where the derivative $\partial/\partial t$ is caused by the transmit antenna and c_0 is the velocity of light. The term $h_{Ch}(t, r)$ is an attenuation term that attenuates the wave and delays it according to the distance. In the frequency domain equation (1) becomes

$$E(f, r) = \underbrace{\frac{1}{r}\exp\left[\frac{-j2\pi fr}{c_0}\right]}_{H_{Ch}(f,r)} H_A(f)\frac{1}{2\pi c_0}j\omega P(f), \qquad (2)$$

where $H_A(f)$ is the antenna transfer function, $P(f)$ is the spectrum of $p(t)$, and the term $j\omega = j2\pi f$ results from the differentiation in the time domain. $H_{Ch}(f, r)$ is the phase shift and attenuation provoked by $h_{Ch}(t, r)$.

From equation (2), the effect on the signal spectrum of the frequency-dependent behavior of the UWB antenna and generated pulse can be schematically shown as depicted in Fig. 5.

https://doi.org/10.1017/S1759078710000310 Published online by Cambridge University Press

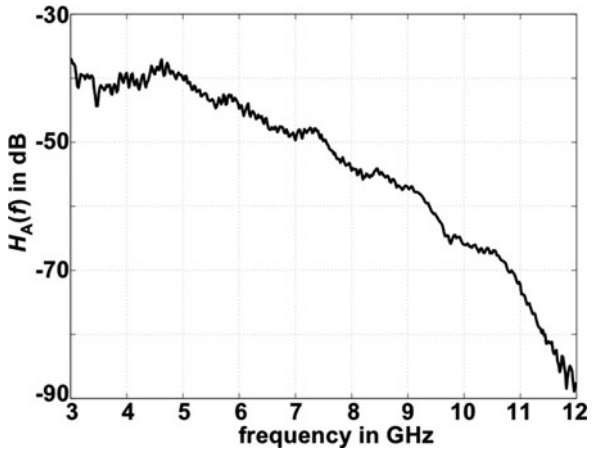

Fig. 4. Measured transfer function of the investigated Bow-tie antenna (co-polarization component, main beam direction).

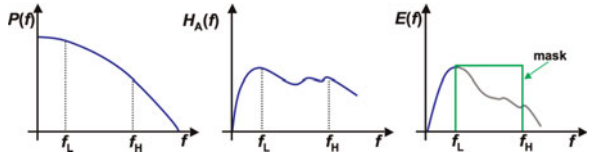

Fig. 5. Effect of the non-ideal behavior of the transmitter. Left: spectrum of the generated pulse. Center: antenna transfer function. Right: resulting transmitted wave versus required mask.

Here the spectrum $P(f)$ of the generated pulse is plotted (left) together with the non-ideal antenna transfer function (center). The generated pulse decreases with frequency, since it is not possible to generate an ideally short pulse with an infinitely large bandwidth, while the antenna transfer function is not constant in the UWB frequency range, i.e. its gain is frequency dependent. The resulting transmitted wave is plotted on the right side of Fig. 5, together with the required mask. Due to the non-ideal behavior of the components, the on-air transmitted wave does not fulfill the given mask.

From this analysis it can be evinced that an optimization process is necessary in order that the radiated wave perfectly fulfills the given mask.

III. SPECTRUM OPTIMIZATION TECHNIQUES

Methods for spectrum optimization can be implemented both digitally and analogically. Classical digital methods consist in designing a particular pulse shape applying windowing realized through FIR or IIR filters [3–6]. The higher the coefficients of the filter, the most the obtained pulse matches the desired mask. For example in [6] an order 66 FIR filter is required to obtain a spectral efficiency of at least 80%. Hence, these methods require high computational efforts. Because of that, analog methods are regarded in the following.

The method, which is used in the following, consists in realizing an *ad hoc* analog filter, whose aim is to pre-distort the signal in order to compensate for the frequency-dependent behavior of the UWB RF-front end. The operational method for designing the required filter transfer function $H_F(f)$, which permits the transmitted signal to optimally exploit the given mask at the antenna output, is now shown. The purpose of such a filter is double: firstly, it has to select the frequency interval of interest (e.g. for the EU-UWB regulation, the 6–8.5 GHz frequency interval); secondly, it has to predistort the signal in order to compensate for the frequency-dependent behavior of the $P(f)$ and $H_A(f)$. Because of that this filter has been referred as "shaping filter." The system block scheme after the application of the shaping filter is shown in Fig. 6, where $E_{UWB}(f)$ is the desired spectrum of the radiated wave at the antenna output, which perfectly fulfills the given mask.

Since the mask has to be satisfied at the antenna output, the radiated electric field $E(f, r)$ is normalized so that the dependence on the distance can be neglected, i.e. only relative values of PSD are considered, which are normalized to the distance r, namely

$$E(f) = \frac{E(f, r)}{H_{Ch}(f, r)}. \tag{3}$$

From Fig. 6, $E_{UWB}(f)$ is given by

$$E_{UWB}(f) = H_A(f)H_F(f)\frac{1}{2\pi c_0} j\omega P(f), \tag{4}$$

where $H_A(f)$ is assumed the antenna transfer function in the main beam direction, co-polarization. From the above equation, the required filter transfer function can be derived, namely

$$H_F(f) = \frac{E_{UWB}(f)}{H_A(f)\left(1/2\pi c_0\right) j\omega P(f)}. \tag{5}$$

It has to be noted that, comparing equation (5) with equation (2), the denominator of equation (5) is exactly the transmitted wave in the case where no filter are applied, namely

$$H_F(f) = \frac{E_{UWB}(f)}{E(f)}. \tag{6}$$

This process is illustrated in Fig. 7. On the left-hand side, the spectrum of the required on-air transmitted wave is shown, together with the spectrum of the actually on-air transmitted wave. On the right-hand side, the required filter transfer function is shown. It can be seen that the shaping filter has to show a band-selection behavior, in order to select the required frequency interval. Moreover, the in-band transfer function is not constant, as for classical bandpass filters, rather it increases with the frequency, i.e. it is frequency-dependent. This permits to compensate for the frequency-dependent behavior of the RF-front end.

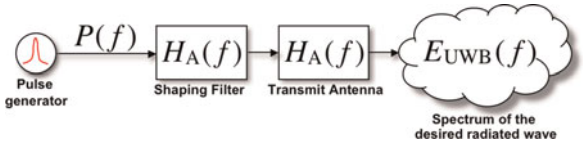

Fig. 6. System block scheme for spectrum optimization (frequency domain representation).

https://doi.org/10.1017/S1759078710000310 Published online by Cambridge University Press

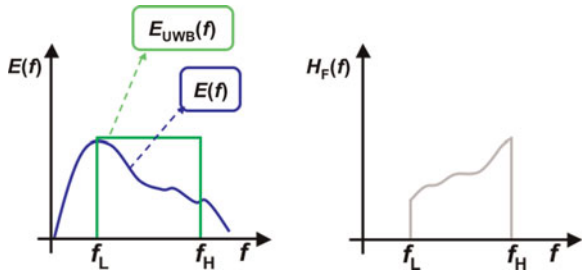

Fig. 7. Shaping filter transfer function design.

IV. PRACTICAL METHODS FOR THE REALIZATION OF SHAPING FILTERS

In practical filter realizations, it is difficult to obtain such a frequency-dependent behavior. Hence, an approximation has to be introduced. Instead of the actually measured $E(f)$, in equation (6) its linear approximation $E_{Approx}(f)$ is used. The approximate filter transfer function becomes

$$H_{F,\,Approx}(f) = \frac{E_{UWB}(f)}{E_{Approx}(f)}. \qquad (7)$$

This process is schematically shown in Fig. 8.

The obtained shaping filter transfer function is hence monotonically increasing in its passband (i.e. in the UWB frequency interval). The slope is directly proportional to the decrement in the UWB frequency interval of the spectrum of the radiated wave, because of the decreasing pulse spectrum and the antenna transfer function as the frequency increases.

In the following, practical methods to realize shaping filters are addressed.

A) Cascade shaping filters

A first method to realize shaping filters consists in creating a cascade of a bandpass section and of a shaping section so that the two tasks of a shaping filter (band selection and pre-distortion) are divided into two different units. The bandpass section can be realized with conventional methods (microstrip resonator stubs, coupling lines, etc. [14, 15]). The shaping section can be produced in different ways. A practical method consists in realizing it through a highpass section, whose lower cut-off frequency coincides with the highest frequency in the selected interval (e.g. for the EU-UWB regulation $f_{cutoff} = f_H = 8.5$ GHz). In this case, the frequency-dependent filter transfer function is obtained by the transitional band of the highpass section. An example of a shaping filter realized in this way is given in [11].

B) Integrated shaping filters

The second typology of shaping filter consists in realizing directly the band selection and the pre-distortion operation in a unique section integrating these two operations in a single unit. This permits to avoid spurious reflections due to the cascade connection in the previous model. This can be achieved by the integration of a highpass section, to obtain the shaping, and a lowpass section, to define the upper range of the frequency interval, in a single unit.

V. EXAMPLE OF SHAPING FILTER REALIZATION

In this section, an example of the previous method is applied to a specific scenario to verify the method itself. The aim is to optimize the spectrum of the on-air radiated signal such that it matches the EU-UWB mask.

A) Investigated scenario

The investigated scenario is composed by a commercially available pulse generator (PSPL 3600 [12], see Fig. 2), a Bow-tie antenna (see Figs 3 and 4, which is optimized for the UWB range), a horn antenna (used at the receiver side, Model 3600). The data received by the horn antenna are acquired by a real-time oscilloscope (Agilent Infinium, 12 GHz bandwidth, 40 GS/s) and recorded and processed by a laptop. The synchronization between the pulse generator and the oscilloscope is done by a trigger source (Textronik, Arbitrary Waveform Generator, pulse repetition frequency 10 kHz). Two measurements have been made: firstly, with a direct connection between the pulse generator and the antenna; secondly, with the shaping filter in between. The investigated scenario is shown in Fig. 9.

Through a direct connection of the pulse generator and the Bow-tie antenna (Fig. 9, solid line), the radiated wave $E(f)$ can be recovered. It is shown in Fig. 10 together with its linear approximation. Here, the effect of the connecting cables, of the horn receive antenna and of the distance between the transmit and receive antennas, have been calibrated. The linear approximation of the measured data is inserted in equation (6) for the shaping filter synthesis. The so obtained

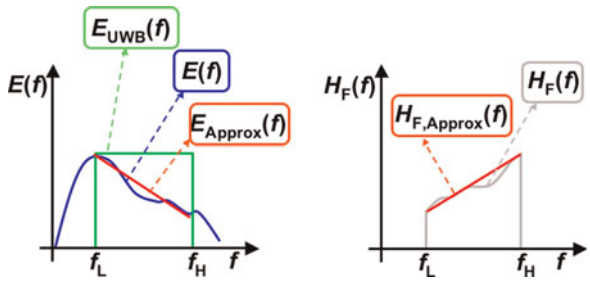

Fig. 8. Approximate shaping filter transfer function design.

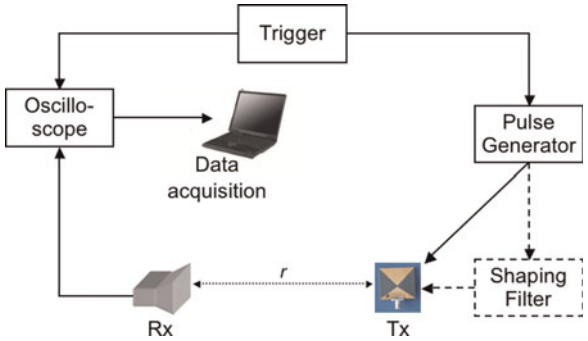

Fig. 9. Block scheme of the investigated scenario.

https://doi.org/10.1017/S1759078710000310 Published online by Cambridge University Press

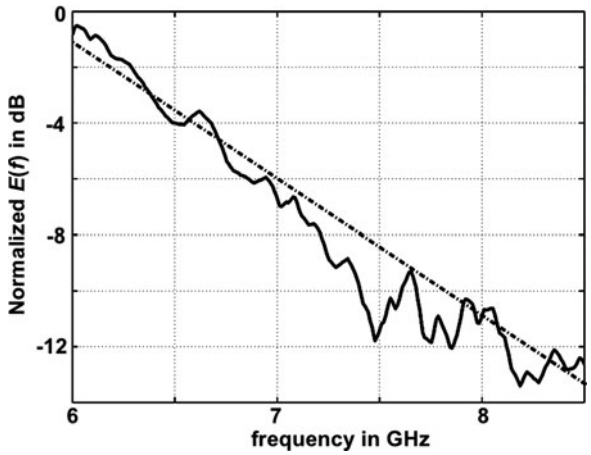

Fig. 10. Normalized measured spectrum $E(f)$ of the transmitted wave.

required approximated shaping filter transfer function is shown in Fig. 11.

B) Realized shaping filter

The fabricated shaping filter consists of a coplanar waveguide (CPW) structure, which is composed by the integration of a highpass section and a lowpass section. The highpass section consists of the integration of two different CPW elements with highpass behavior: the open-end series stub and the short-end shunt stub [16, 17]. These elements are integrated one into the other for space reduction. The lengths of the stubs have been optimized to obtain the desired slope in the passband. The lowpass section has been realized through a short-end series stub and a defected ground plane structure. The defected ground plane structure has been realized through slots etched symmetrically in the CPW ground plane [16]. The slots have been bended for space reduction. This basic structure has been repeated twice to obtain a sharper upper transitional band. A prototype of this filter has been etched on the substrate Roger RO4003, $\varepsilon_r = 3.38$, and thickness $h = 1.57$ mm (see Fig. 12). The measured transfer function of the realized filter is shown in Fig. 13.

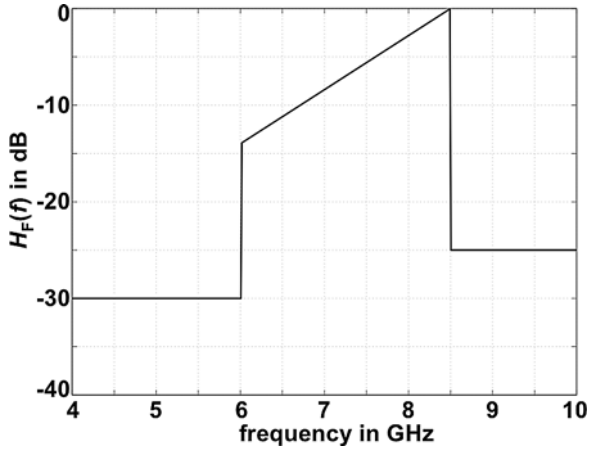

Fig. 11. Mask of the required mask of the shaping filter for the investigated scenario.

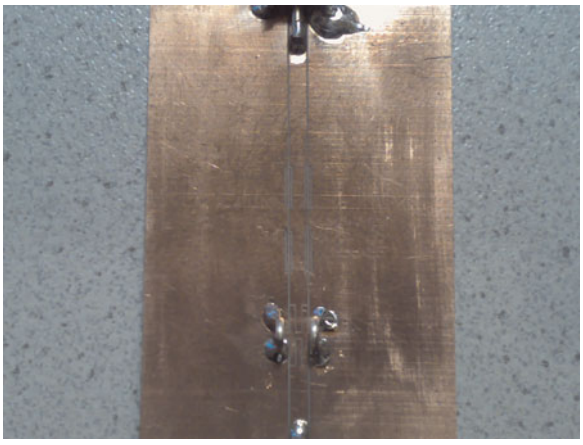

Fig. 12. Fabricated prototype of the required shaping filter.

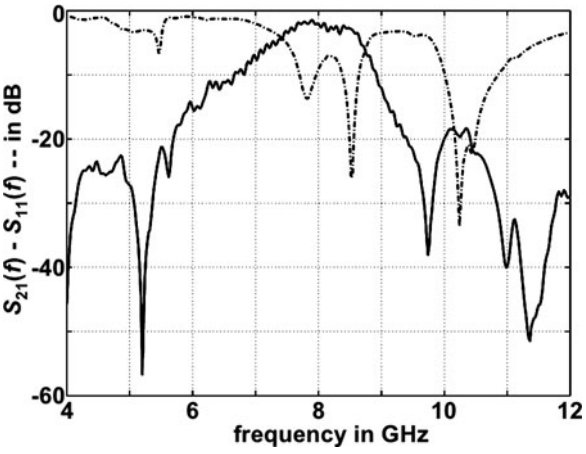

Fig. 13. Measured $S_{21}(f)$ (solid line) and $S_{11}(f)$ (dotted line) parameters of the realized shaping filter.

The normalized recovered PSD of the radiated wave is shown in Fig. 14. It can be recognized that the shaping filter permits a better exploitation of the in-band spectrum, i.e. the mask is better fulfilled w.r.t. the case when no filter is applied (see Fig. 10). In order to quantify the system performance improvement by the application of the shaping filter with

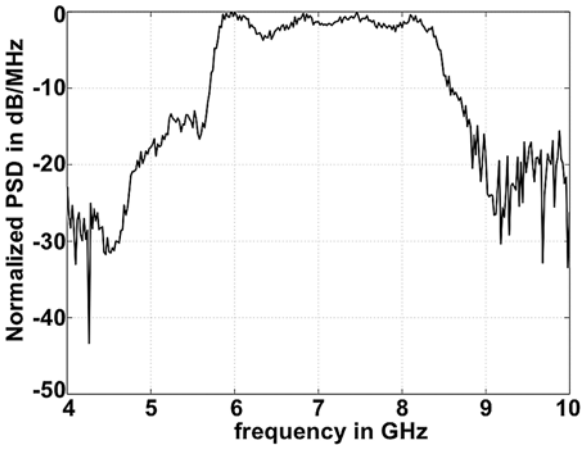

Fig. 14. Normalized PSD of the radiated wave with shaping filter.

https://doi.org/10.1017/S1759078710000310 Published online by Cambridge University Press

Table 1. Computed efficiency from measurement results.

No filter	Bandpass filter	Shaping filter
1.6%	38.2%	58.2%

respect to (w.r.t.) the classical bandpass filters, the efficiency of the system has been calculated. This has been done by integrating the PSD of the signal in the passband interval 6–8.5 GHz and comparing the result to the integral of the PSD of an ideal signal having a rectangular spectrum in the 6–8.5 GHz interval and a maximum value equal to the maximum value of the spectrum of the measured signal in that band. The obtained results are summarized in Table 1. The case "No-Filter" refers to the measurement with a direct connection between the pulse generator and the antenna. In this case, in order to respect the mask, the power of the transmitted signal has to be lowered. The case "Bandpass-Filter" represents the signal, which would be radiated if only an ideal rectangular bandpass filter (i.e., it only selects the frequency interval) would be inserted in between the antenna and the pulse generator.

From the obtained results, it can be concluded that the application of the shaping filter permits to obtain a considerable improvement of system performance, since the mask is better fulfilled w.r.t. the case when only a bandpass filter is applied.

VI. CONCLUSIONS

In this paper, an analysis of the UWB transmitter RF-front end has been performed in order to investigate how the non-ideal and frequency-dependent behavior of the UWB components affects and distorts the radiated wave.

Different methods for signal optimization have been investigated, both digital and analog. Moreover, an example of spectral system optimization with analogical devices have been shown and verified through measurement results.

ACKNOWLEDGEMENT

This work was supported by COST Action IC0803 "*RF/Microwave communication subsystems for emerging wireless technologies*" (RFCSET).

REFERENCES

[1] Revision of Part 15 of the Commission's Rules Regarding Ultra-Wideband Transmission System, ET-Docket 98-153, FCC, February 14, 2002.

[2] Official Journal of the European Union, 23 February 2007, L.55/33–36.

[3] Yang, L.; Giannakis, G.: Ultra-wideband communications, an idea whose time has come. IEEE Signal Process. Mag., **21**(6) (2004), 26–54.

[4] Parr, B.; Cho, B.; Wallace, K.; Ding, Z.: A novel ultra-wideband pulse design algorithm. IEEE Commun. Lett., **7**(5) (2003), 219–221.

[5] Wu, X.; Tian, Z.; Davidson, T.; Giannakis, G.: Optimal waveform design for UWB radios. IEEE Trans. Signal Process., **54**(6) (2006), 2009–2021.

[6] Timmermann, J.; Rashidi, A.A.; Walk, P.; Pancera, E.; Zwick, T.: Application of optimal pulse design in non-ideal ultra-wideband transmission, in GeMIC2009, March 2009.

[7] Hong, J.-S.; Shaman, H.: An optimum ultra-wideband microstrip filter. Microw. Opt. Technol. Lett., **47**(3) (2005), 230–233.

[8] Pancera, E.; Zwick, T.; Wiesbeck, W.: Compact UWB bandpass filter based on microstrip-to-slotline transitions. J. Eur. Microw. Assoc., **4**(4) (2008), 289–293.

[9] Shaman, H., Hong, J.-S.: Novel ultra-wideband (UWB) bandpass filter with pairs of transmissions zeroes. IEEE Microw. Wirel. Compon. Lett., **17**(2) (2007), 121–123.

[10] Soergel, W.; Wiesbeck, W.: Influence of the antennas on the ultra-wideband transmission. EURASIP J. Appl. Signal Process., **3** (2005), 296–305.

[11] Pancera, E.; Timmermann, J.; Zwick, T.; Wiesbeck, W.: Filter design for spectrum optimization in ultra wideband systems, in ICUWB09, September 2009.

[12] Picosecond Pulse Labs, Model PSPL3600 Impulse Generator Instruction Manual.

[13] Farr, E.; Baum, C.; Buchenauer, C.J.: Impulse radiating antennas, Part II, in Carin, L.; Felsen, L.B. (eds.), Ultra Wideband Short Pulse Electromagnetics, vol. **2**, Plenum Press, New York, 1995.

[14] Matthaei, G.; Young, L.; Jones, E.: Microwave Filters, Impedance Matching Networks and Coupling Structures, Artech House, Norwood, MA, 1980.

[15] Hong, J.S.; Lancaster, M.J.: Microstrip Filters for RF/Microwave Applications, John Wiley and Sons, Inc., New York, 2001.

[16] Simons, R.N.: Coplanar Waveguide Circuits, Components, and Systems, John Wiley & Sons, Inc., New York, 2001.

[17] Dib, N.I.; Ponchak, G.E.; Katehi, L.P.B.: A theoretical and experimental study of coplanar waveguide shunt stubs. IEEE Trans. Microwave Theory Tech., **41** (1) (1993), 38–44.

[18] Wiesbeck, W.; Adamiuk, G.: Antennas for UWB systems, in INICA07, March 2007.

Elena Pancera was born in 1981 in Verona, Italy. She graduated in 2005 (summa cum laude) in Telecommunications Engineering at the University of Padova, Italy. She collaborated with the Department of Information Engineering at the same University, working at a PRIN Project (Research Project of Relevant National Interest) dealing with UWB systems. In 2007 she jointed the Institut für Hochfrequenztechnik und Elektronik (IHE), Karlsruhe Institute of Technology (former Universität Karlsruhe (TH)), Germany, where she obtained her Dr.-Ing. (Ph.D.E.E.) in 2009 (summa cum laude). Actually she is a research assistant at the same Institute. Her main research interests are UWB systems and in particular UWB antennas and filters, UWB system optimization and UWB radar. She serves as a teacher for courses organized by the "*European School of Antennas*." She is the leader of the Focus Area "*Impulse Radio UWB System*" in the COST Action IC0803 "*RF Microwave Communication Subsystems for Emerging Wireless Technologies*."

https://doi.org/10.1017/S1759078710000310 Published online by Cambridge University Press

Jens Timmermann was born in 1981 in Heidelberg, Germany. He studied electrical engineering at the University of Karlsruhe, Germany, and received the diploma degree in September 2006. From October 2006 to December 2009, he was with the Institut fuer Hoechstfrequenztechnik und Elekronik at the same University, working in the field of ultra-wideband communications with focus on the influence of non-ideal system components such as antennas, channel, and filters. Mr. Jens Timmermann received the Dr.-Ing. (Ph.D.E.E.) in December 2009. Since 2010, he is with EADS Astrium, Friedrichshafen, Germany, in the field of next generation atomic clocks for the International Space Station ISS.

Thomas Zwick received the Dipl.-Ing. (M.S.E.E.) and the Dr.-Ing. (Ph.D.E.E.) degrees from the Universität Karlsruhe (TH), Germany in 1994 and 1999, respectively. From 1994 to 2001 he was a research assistant at the Institut für Höchstfrequenztechnik und Elektronik (IHE) at the Universität Karlsruhe (TH), Germany. February 2001 he joined IBM as Research Staff Member at the IBM T. J. Watson Research Center in Yorktown Heights, NY, USA. From October 2004 to September 2007 T. Zwick was with Siemens AG, Lindau, Germany. During this period he managed the RF development team for automotive radars. In October he became appointed as full professor at the Universität Karlsruhe (TH), Germany. T. Zwick is a director of the Institut für Hochfrequenztechnik und Elektronik (IHE) at the Karlsruhe Institute of Technology (former Universität Karlsruhe (TH)), Germany. His research topics include wave propagation, stochastic channel modeling, channel measurement techniques, material measurements, microwave techniques, millimeter wave antenna design, wireless communication, and radar system design. He participated as an expert in the European COST231 *Evolution of Land Mobile Radio (Including Personal) Communications* and COST259 *Wireless Flexible Personalized Communications*. For the Carl Cranz Series for Scientific Education he served as a lecturer for *Wave Propagation*. He received the best paper award on the Intern. Symp. on Spread Spectrum Techn. and Appl. ISSSTA 1998. In 2005 he received the Lewis award for outstanding paper at the IEEE International Solid State Circuits Conference. Since 2008 he is president of the Institute for Microwaves and Antennas (IMA). T. Zwick is author or co-author of over 80 technical papers and over 10 patents.

Werner Wiesbeck received the Dipl.-Ing. (M.S.E.E.) and the Dr.-Ing. (Ph.D.E.E.) degrees from the Technical University Munich in 1969 and 1972, respectively. From 1972 to 1983 he was with AEG-Telefunken. From 1983 to 2007 he was director of the Institut für Höchstfrequenztechnik und Elektronik (IHE) at the University of Karlsruhe (TH), and he is now Distinguished Scientist at the Karlsruhe Institute of Technology. Research topics include electromagnetics, antennas, wave propagation, communications, and radar and remote sensing. He has been a member of the IEEE GRS-S AdCom (1992–2000), in various positions, including President IEEE GRS-S (2000–2001). He has been General Chairman of the '88 Heinrich Hertz Centennial Symposium, the '93 Conference on Microwaves and Optics (MIOP '93), the Technical Chairman of International mm-Wave and Infrared Conference 2004, Chairman of the German Microwave Conference GeMIC 2006. He is the recipient of a number of awards, lately the IEEE Millennium Award, the IEEE GRS-S Distinguished Achievement Award, the Honorary Doctorate (Dr. h.c.) from the University Budapest/Hungary, the Honorary Doctorate (Dr.-Ing. E.h.) from the University Duisburg/Germany and the IEEE Electromagnetics Award 2008. He is a Fellow of IEEE, an Honorary Life Member of IEEE GRS-S, a Member of the Heidelberger Academy of Sciences and a Member of acatech (German Academy of Engineering and Technology).

https://doi.org/10.1017/S1759078710000310 Published online by Cambridge University Press